The Geological Evolution of the Tibetan Plateau

Leigh H. Royden,* B. Clark Burchfiel, Robert D. van der Hilst

The geological evolution of the Tibetan plateau is best viewed in a context broader than the India-Eurasia collision zone. After collision about 50 million years ago, crust was shortened in western and central Tibet, while large fragments of lithosphere moved from the collision zone toward areas of trench rollback in the western Pacific and Indonesia. Cessation of rapid Pacific trench migration (~15 to 20 million years ago) coincided with a slowing of fragment extrusion beyond the plateau and probably contributed to the onset of rapid surface uplift and crustal thickening in eastern Tibet. The latter appear to result from rapid eastward flow of the deep crust, probably within crustal channels imaged seismically beneath eastern Tibet. These events mark a transition to the modern structural system that currently accommodates deformation within Tibet.

Commonly referred to as the "Roof of the World," the Tibetan plateau stands 5 km high over a region of approximately 3 million km^2 (Fig. 1). As early as the 1920s, Argand (*1*) postulated that the plateau formed as the result of collision and postcollisional convergence of the Indian subcontinent with Eurasia, causing shortening and thickening of the crust to ~80 km and producing the magnificent mountain ranges of the Himalaya, Karakorum, and Tien Shan. This perspective remains widely accepted, but the development of the plateau can also be evaluated within the context of the large dynamic system related to subduction of oceanic lithosphere beneath eastern Eurasia and Indonesia.

Despite decades of study, controversy remains over basic aspects of Tibetan geology. For example, the mantle lithosphere beneath Tibet has been proposed to be cold, hot, thickened by shortening, or thinned by viscous instability. Other controversies include the degree of mechanical coupling between the crust and deeper lithosphere and the nature of large-scale deformation (*2*–*4*). The Tibetan lithosphere is complex, composed of fragments of different ages, compositions, temperatures, and rheology. Understanding the processes that have formed the plateau requires reconstruction of changing patterns of deformation and uplift across a wide range of temporal and spatial scales.

Precollisional Tectonics (Before ~50 Ma)

The development of high topography and thickened crust in the Tibetan region began before continental collision, during subduction of the Tethys oceans northward beneath Eurasia. Early Cretaceous thrust faulting, folding, and crustal thickening took place along the Bangong suture in what is now central Tibet. In Late Cretaceous to Early Eocene time, an Andean mountain range with abundant magmatic activity and a back-arc thrust belt developed along the southern margin of the Eurasian plate (*5*) (Fig. 2).

By Late Cretaceous time, the southern and central plateau was elevated above sea level, which suggests thickening of the continental crust, but northern and northeastern Tibet contained broad areas of nonmarine, and locally marine, deposition, which indicates little crustal thickening there. Plate reconstructions at the time of collision, ~50 million years ago (Ma) (*6*, *7*), place the Indian subcontinent ~2500 km south of its current position (Fig. 3). Estimates of subsequent shortening within the central Himalaya suggest that ~500 to 1000 km of Indian continental lithosphere existed northward of what is now north-central India (*8*).

Through much of Late Cretaceous time, the trenches of the western Pacific subduction boundaries rolled back slowly. This produced north-south trending extension in east China and adjacent offshore areas (*9*), but there is little evidence for eastward movement of continental lithosphere away from southeastern Tibet before collision.

Early Cenozoic Tectonics (~50 Ma to ~20 Ma)

After collision, intracontinental convergence and deformation continued across Tibet, reaching

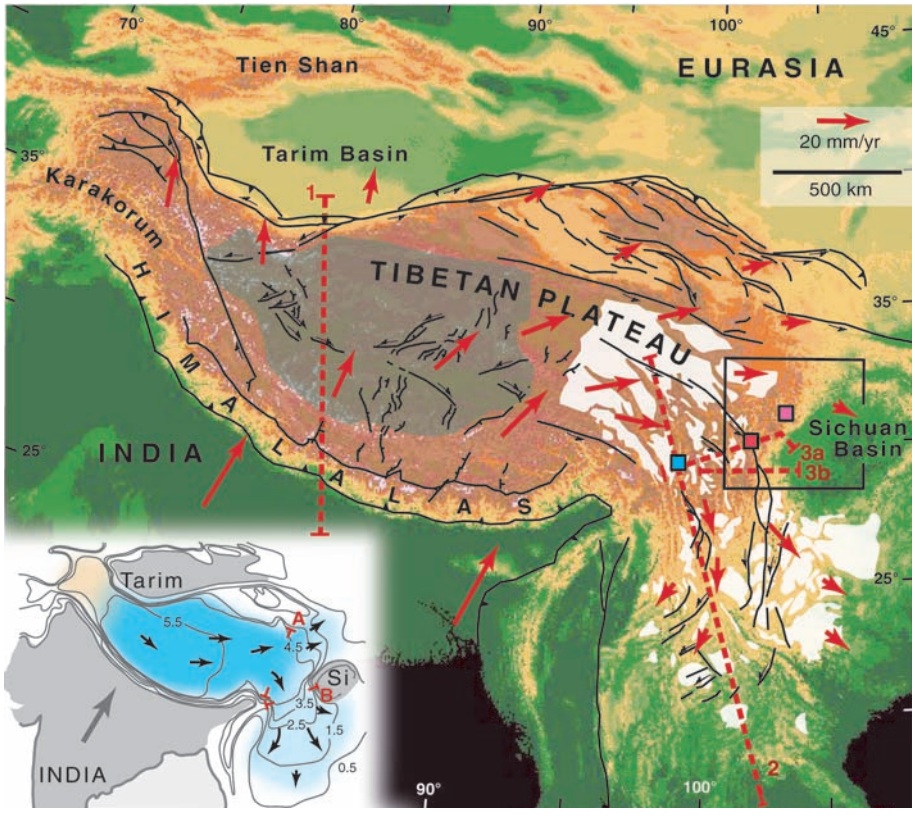

Fig. 1. Topography shade map for the Tibetan region showing the relict landscape of eastern Tibet (white shading) and internally drained region of central Tibet (gray-green shading). Red arrows are selected and slightly generalized GPS measurements (*22*, *24*). Red dashed lines are cross-section locations for Fig. 5; box outlined in black is location of Fig. 6; black lines are young geologic structures; colored squares are ages of initiation of rapid river incision (pink, 5 to 12 Ma; blue, 10 to 15 Ma; red, 8 to 10 Ma) (*34*–*36*). Inset shows the approximate area of deep crustal flow (blue shading) with topographic contours (1-km interval from 500 m) and section lines (A and B) used to constrain rates of deep crustal flow. Black arrows are inferred direction of lower crustal flow (*38*), Si, Sichuan Basin.

Department of Earth, Atmospheric, and Planetary Sciences, Massachusetts Institute of Technology, Cambridge, MA 01890, USA.

*To whom correspondence should be addressed. E-mail: lhroyden@mit.edu

northward to involve a larger area than previously (Fig. 2). In the central Himalaya, postcollisional deformation involved south-vergent thrusting and folding of rocks of the north Indian passive margin as it was subducted beneath Eurasia. Concurrently, crustal shortening formed mostly narrow basins in central and southern Tibet with thick nonmarine, syntectonic strata, bounded by thrust faults that dip south and, more commonly, north (*10*). The magnitude of this Early Cenozoic shortening is unknown; within the basins, shortening is small but locally may reach more than 50%. It has been suggested that this shortening reflects the beginning of southward underthrusting of Eurasia below Tibet (*11*, *12*). Oxygen isotope data suggest that as early as Eocene/Oligocene time the southern and central part of the Tibetan plateau had reached high elevations, whereas the northern part of the plateau remained low (*13*).

At this time, large fragments of Eurasian lithosphere were extruded eastward out of central Tibet, from the Bangong suture region toward southern China and northern Indochina (*2*, *14*) (Fig. 3). The similarity between Eocene folded strata in northern Indochina and central Tibet indicates that these continental fragments were deformed after collision but before or during extrusion. Deformation may have been facilitated by very high lithospheric temperatures, as expressed by a belt of alkali-rich magmatic rocks erupted between ~30 and ~50 Ma (more were erupted later) with melt temperatures of ~1300°C to 1400°C at depths of 80 to 100 km (*15*). In the east, the distribution of these magmatic rocks corresponds closely with that of the extruded fragments.

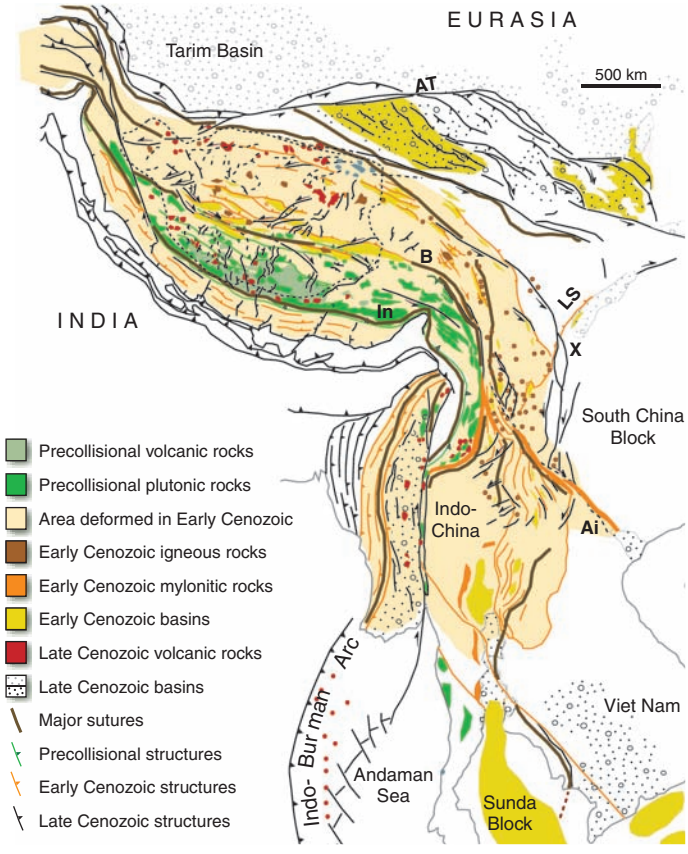

Fig. 2. Tectonic map of Tibet and adjacent regions showing distribution of major structures and rock units grouped approximately into precollisional (before ~50 Ma), Early Cenozoic (before ~20 Ma), and Late Cenozoic (after ~20 Ma). In, Indus suture; B, Bangong suture; LS, Longminshan thrust belt; X, Xianshuehe fault system; Ai, Ailao Shan; AT, Altyn Tagh fault.

The Ailao Shan shear zone (Fig. 2) probably formed the northern boundary of the east-moving fragments (*2*) until the Altyn Tagh fault became active in the late part of the Early Cenozoic. Left-slip on the Altyn Tagh fault was transferred into shortening in the northeastern plateau, probably beginning by Oligocene time when nonmarine rocks, previously deposited in broad basins connected with the Tarim Basin, began to be confined to local basins (*10*, *11*).

Eastward extrusion of lithosphere from central Tibet occurred during a time of rapid trench rollback along much of the Pacific, Philippine, and Indonesian oceanic subduction boundaries (*2*, *16*). This is documented by widespread Early Cenozoic extension within the upper plate lithosphere of Indonesia (*17*), Eocene-Oligocene extension in the South and East China Seas (*18*), and Early Miocene extension in the Sea of Japan (*19*). Rapid fragment extrusion did not continue past ~15 to 20 Ma, when slab rollback and upper plate extension slowed or ended in most places (*16*).

P-wave tomography reveals a seismically fast structure up to ~400-km depth beneath the southern plateau and northern India (*20*, *21*) (Figs. 4 and 5, profile 1). This broad structure differs from the narrow oceanic slabs imaged beneath the western Pacific; it probably represents subducted continental mantle lithosphere of India. West of ~85°E, its cross-sectional area is consistent with subduction and stacking of ~1000 km of Indian continental lithosphere. East of 85°E, the smaller cross-sectional area indicates that less continental lithosphere may have been subducted here.

Late Cenozoic Tectonics (After ~15 to 20 Ma)

As India-Eurasia convergence continued into Late Cenozoic time, southward thrusting continued in the middle and lesser Himalaya, in-

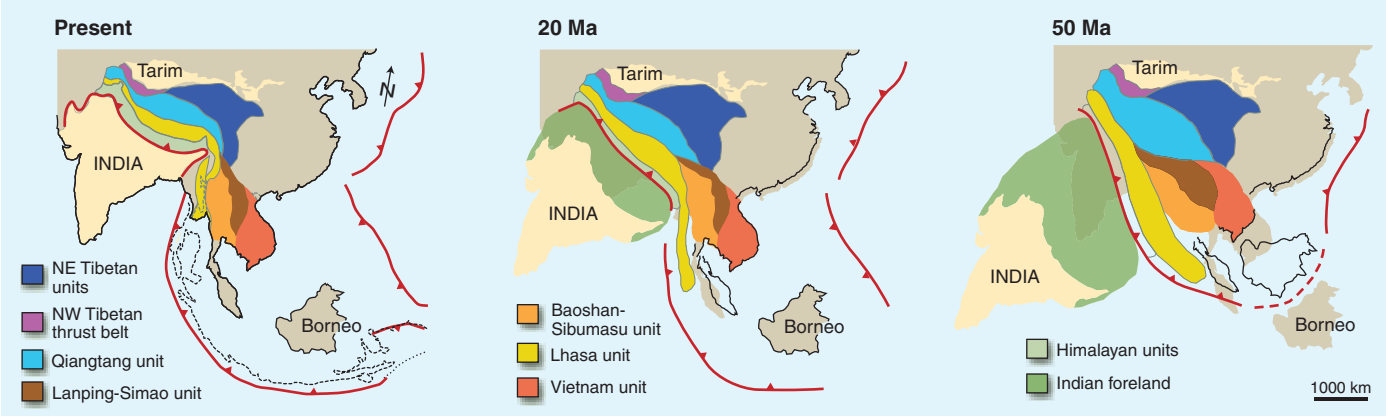

Fig. 3. Tectonic reconstructions around the time of collision (~50 Ma) and at 20 Ma, with India and Eurasia positions determined from sea-floor magnetic anomalies (*6*). Major tectonic units of Tibet and Indochina are generalized by color; their reconstructed shapes are estimates and are poorly known. Bold red lines are estimated positions of subduction zones. Light brown shows the present distribution of land areas.

volving deeper parts of the Indian crust (Fig. 2). North of the Himalaya, the pattern of large-scale deformation changed substantially after the Early Cenozoic, with rapid surface uplift of the eastern plateau and the onset of east-west extension in the central plateau. Some shortening still occurred within narrow basins of the central plateau (*13*), but most shortening relocated to northeastern Tibet and to the Tien Shan.

The timing and structural pattern of young faults and Global Positioning System (GPS) data indicate that the modern deformation regime was established by ~15 Ma in central Tibet and by ~8 to 10 Ma in eastern Tibet (*22*, *23*), with north-south shortening, east-west extension, and eastward motion occurring in the southern and central plateau region (*22*, *24*), and shortening in northeastern Tibet. Evidence for Late Cenozoic crustal shortening in eastern and southeastern Tibet is largely absent. Shortening structures of this age are found only along the Longmenshan thrust belt (*25*, *26*), with total displacements of tens of kilometers and active rates less than a few millimeters per year.

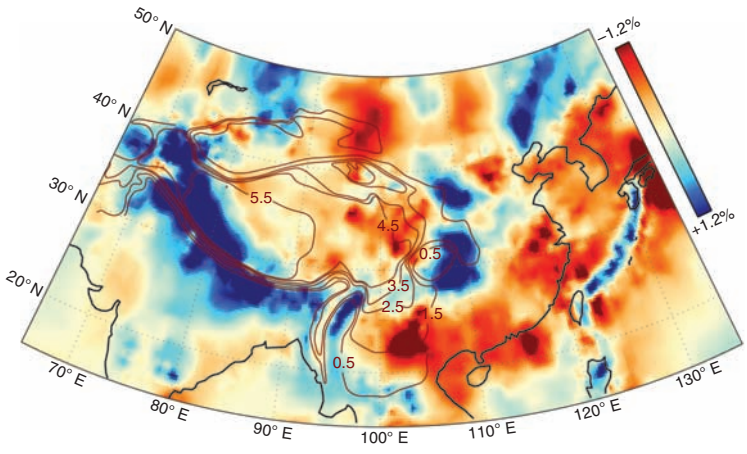

Fig. 4. Lateral variation in *P*-wave speed, at 200-km depth, relative to a laterally homogeneous reference Earth model. This image is part of a global model obtained through tomographic inversion of *P*-wave arrival time data from global, national, and regional seismograph networks (*20*, *21*). The topographic contours (dark red) outline the Tibetan plateau and adjacent areas at elevations from 0.5 to 5.5 km above sea level.

Through the Late Cenozoic, lithospheric fragments continued to be extruded outside the plateau and toward South China and Indochina (*22*). The rates of extrusion were slower than in the Early Cenozoic, but motion was still toward the location of coeval trench rollback along adjacent oceanic subduction boundaries. This is clearest for the Indo-Burman region where upper-plate extension documents westward trench migration beginning at ~20 Ma (*17*). Rapid eastward motions still occurred within the plateau, but most of this motion did not extend outside the plateau. For example, left-slip on the Altyn Tagh fault was transferred into thrust faulting and folding in northeastern Tibet (*27*). Here, narrow high mountain ranges formed and separated deep narrow basins with nonmarine deposition, possibly accompanied by southward subduction of Eurasian crust below central Tibet (*2*, *12*).

To the east, the eastward-moving upper crust of the central and eastern plateau is diverted northeast and southeast around the Sichuan Basin. Marked by fast *P*-wave propagation to at least 250-km depth, this basin appears to be a deeply rooted, mechanically strong unit underlain by craton-like lithosphere that has resisted the multiple deformations that affected the surrounding regions (Fig. 4). Slow seismic-wave propagation in the lithosphere beneath eastern

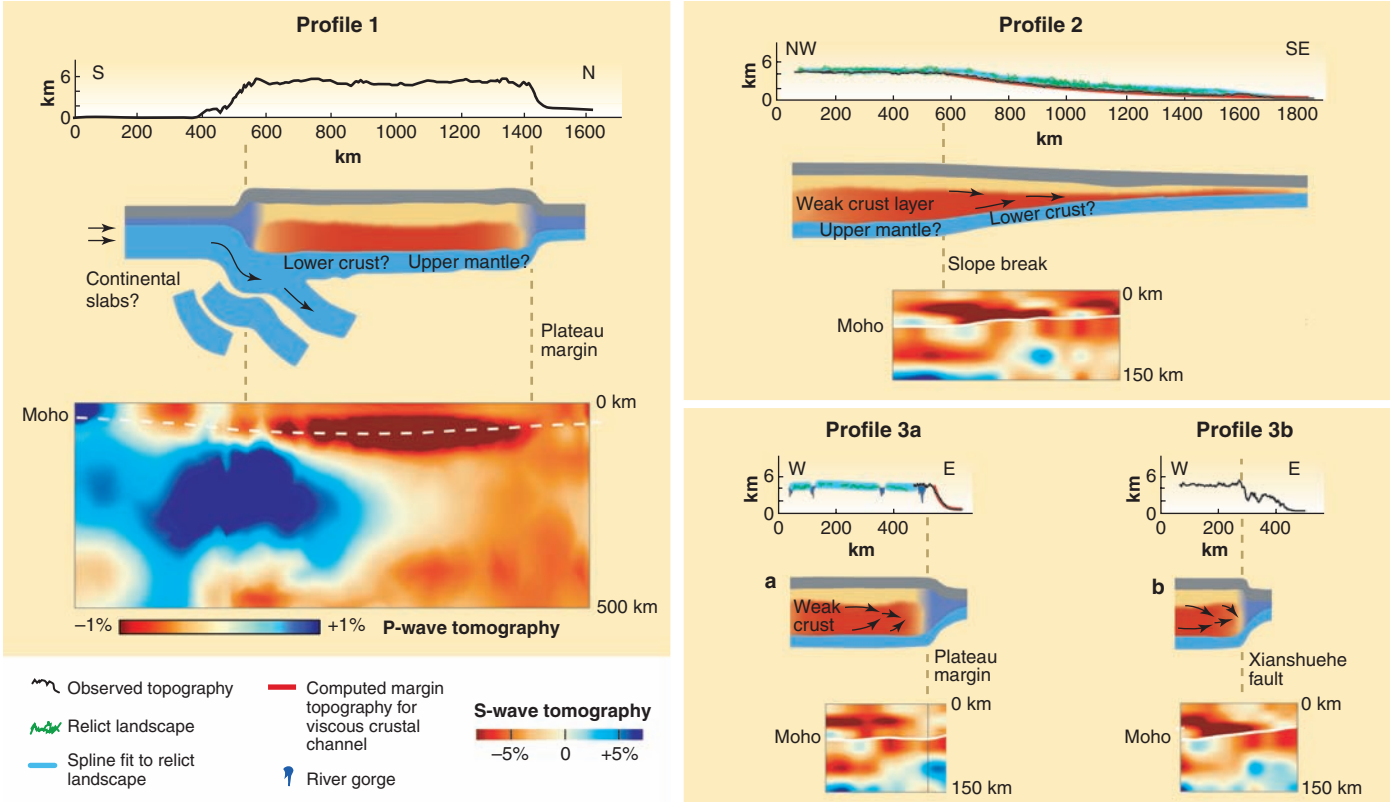

Fig. 5. Profiles through the Tibetan plateau region showing topography (top), conceptual crustal model (middle), and seismic section (bottom). Velocity anomalies are *P*-wave speed on profile 1 and *S*-wave speed on profiles 2, 3a, and 3b (*47*). Moho position is poorly constrained on profile 1, but well constrained from receiver function analysis (*42*) on profiles 2, 3a, and 3b. Profile locations are shown in Fig. 1.

Tibet suggests that its mechanical strength is much lower than beneath the Sichuan Basin.

West and southwest of the Sichuan Basin, southward motion of the upper crust is accommodated by clockwise rotation and by left-slip along the Xianshuihe fault system, which became active at ~8 to 10 Ma and has a net displacement of ~70 km and GPS-measured rates of ~10 to 12 mm/year (*22*–*24*). Southward, near the Ailao Shan, its displacement remains uniform but occurs across a zone 100 km wide without identifiable faults. Northwest of the Sichuan basin, Tibetan upper crust also deforms and moves relative to the basin across a wide area without identifiable faults (*28*). Both regions of active shear without recognized faulting are marked by low seismic-wave speeds, and presumably high temperatures, at ≤200-km depth (*20*) (Fig. 4).

One of the most conspicuous changes in Late Cenozoic deformation is the onset of east-west crustal extension in central Tibet. Extension occurs along north-south trending grabens, northeast-striking left-slip faults and northwest-striking right-slip faults, and reaches southward to include parts of the High Himalaya. Extension may have begun by 13 to 18 Ma and was well under way by 8 Ma (*29*, *30*). The initiation of extension has been proposed to result from rapid removal of Tibetan mantle lithosphere, with a consequent increase in surface elevation of the plateau (*31*), but in our view the initiation of extension is more likely tied to the uplift of eastern Tibet (*32*).

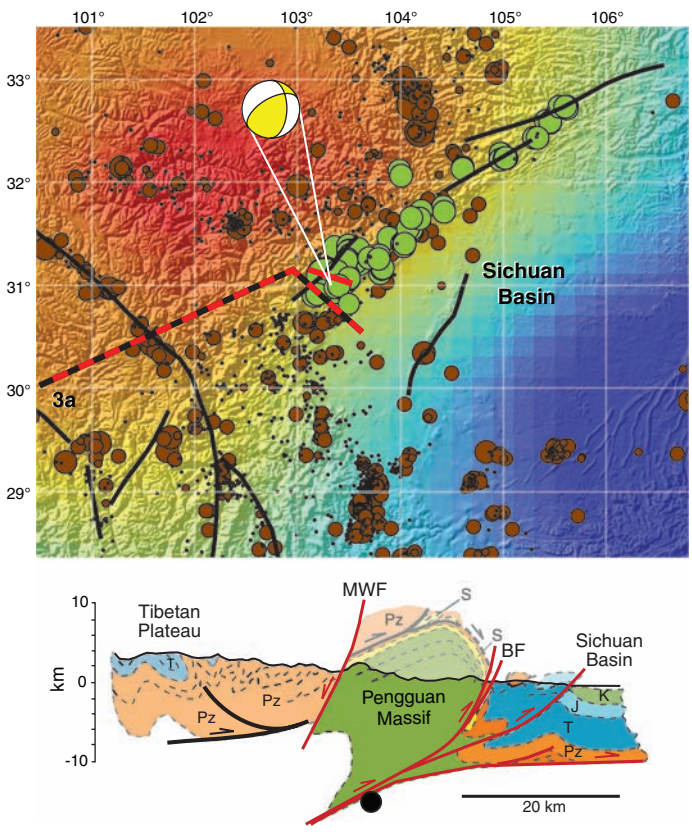

Fig. 6. (**Top**) Epicenters of 12 May 2008 Wenchuan earthquake and aftershocks (green circles), with focal mechanism for the main event (*48*). Events are superimposed on map of lateral variation in *P*-wave speed at 100-km depth relative to a laterally homogeneous reference Earth model (*47*), with color scale the same as in Fig. 4. Brown dots, regional seismicity (body wave magnitude larger than 3, symbol size scaled with magnitude, time interval 1964 to 2007) from EHB catalog (*49*). Map location given in Fig. 1. (**Bottom**) Geological structure along a profile through the hypocenter, modified after (*28*), with location shown by the red line on the map. Black lines, Jurassic faults; red lines, Late Cenozoic faults; S, Sinian (latest Proterozoic); MWF, Maowen-Wenchuan fault zone; BF, southern continuation of the Beichuan fault zone. Partially whited-out structures indicate geologic reconstruction above the modern topographic surface. Yellow circle depicts location of main Wenchuan earthquake with estimated uncertainty in depth of ±5 km.

Tibetan Landscape

The surface of the high central plateau is internally drained, differing considerably from eastern and southeastern Tibet, where a relict landscape is preserved between major rivers (*33*) (Fig. 1). This relict landscape, which extends from the 5-km-high eastern plateau to regions below 1-km elevation, may have been largely established by the end of the Cretaceous; areas deformed in the Early Cenozoic were rebeveled before the Late Cenozoic (*33*). Comparison with modern landscapes suggests that the east Tibetan landscape formed at regional slopes of not more than 10^{-3} to 10^{-4}. Because its downstream end has remained near sea level, where it merges with the modern coastal plain, its upstream portion probably formed at elevations less than ~1.5 km.

The east Tibetan landscape is currently undergoing rapid change as the major rivers that drain the plateau are incising at ~0.3 to 0.4 mm/year (*34*, *35*), carving gorges up to 3 km deep. U-Th/He dating on apatite shows that river incision started at ~8 to 15 Ma on major tributaries of the Yangtze River (*34*, *35*) and at ~5 to 12 Ma along the Longmenshan plateau margin (*36*) (Fig. 1). Thus, uplift of the eastern plateau, the onset of east-west extension in the central plateau, and the structural transition to the modern fault patterns all date to ~10 to 15 Ma, whereas uplift of central Tibet occurred much earlier (*13*).

Crustal Rheology and Dynamics

Much of the active deformation of Tibet results from its high topography. Surface strain rates, inferred from GPS and earthquake data, are consistent with gravitationally driven flow of a viscous lithosphere bounded by stronger converging blocks to the north and south (*4*, *37*, *38*) (Fig. 1). Whether this coherently deforming layer extends into the upper mantle or whether it ends within the crust, thereby allowing for some degree of mechanical decoupling between upper crust and mantle, is a topic of ongoing debate.

Magnetotelluric data from the eastern and south central plateau indicate a hot, fluid-rich middle crust (*39*). In a few localities, young magmatic rocks with melt temperatures of 1300 to 1400°C indicate high temperatures just below and probably within the deeper crust (*15*). Surface-wave tomography (*40*, *41*) and receiver function analysis (*42*) from regional seismic arrays in eastern and southeastern Tibet show a middle and lower crustal network with low shear-wave speed, and presumably low mechanical strength (Fig. 5). These low-velocity zones terminate against the steeply sloping plateau margin adjacent to the Sichuan Basin. These results support model predictions that plateau morphology correlates with the underlying crustal rheology (*38*, *43*, *44*): The high plateau and the gently sloping southeastern and northeastern margins overlie weak crustal zones, and steeply sloping margins overlie crust that is strong throughout.

Arguments for deep crustal flow beneath Tibet come largely from the history of the eastern plateau, which was uplifted without substantial shortening of the upper crust (*23*, *38*). Unless new crust is introduced from the mantle, crustal thickening and surface uplift require rapid eastward flow in the deep crust (Fig. 1), probably within the slow seismic zones imaged in the middle and lower crust, but this interpretation remains controversial. Deep crustal flow would have occurred over distances of hundreds to perhaps 1000 km. A rough volume balance for the past 15 million years suggests that deep crustal flow through profiles A and B (Fig. 1, inset) averaged a minimum of ~70 to 100 mm/year, approximately five times that of the upper crust, with the viscosity of the deep crust being several orders of magnitude smaller than that of the upper crust (*45*).

The cause, formation, and lateral interconnectivity of weak crustal zones beneath Tibet remain unclear. The weak crust is probably hot, an expected consequence of radiogenic heating in a thickened crust, but modeling and surface-wave tomography indicate that weak crust also

extends to low elevations beneath the southeastern margin where the crust has not been greatly thickened. Model studies suggest that the east Tibetan crust became weak before it became thick.

We speculate that until ~15 Ma, a zone of stronger crust supported the eastern margin of the plateau, separating an area of weak lower crust beneath what is now the central plateau from an area of weak lower crust beneath the lowland region that is now eastern Tibet. We further suggest that this plateau margin advanced into eastern Tibet at ~15 to 10 Ma, uniting the areas of weak crust. This enabled rapid eastward flow of deep crust from central Tibet into eastern and southeastern Tibet, along with slower flow in the upper crust and east-west surface extension. In our interpretation, the initiation of east-west extension in central Tibet, the uplift of eastern Tibet, and the establishment of the modern deformation field in central and eastern Tibet are all the result of this process originating in the deep crust.

Conclusions

The evolution of the Tibetan plateau involves subduction of Indian lithosphere, thickening of Tibetan crust, and eastward extrusion of Tibetan lithosphere. Data summarized here indicate that extrusion of lithospheric fragments beyond the borders of the plateau correlates with trench rollback in the western Pacific and around Indonesia. We suggest that both a source (area of thickening crust in central Tibet) and a sink (areas of trench rollback to the east and southeast) are needed to enable large-scale extrusion of lithospheric fragments beyond the borders of the plateau. As a corollary, the slowing and reorganization of oceanic trench rollback in the early part of Late Cenozoic time may have been responsible for the coeval slowing and reorientation of fragment extrusion and may have contributed to eastward growth of the plateau.

We propose that the transformation from the older structural regime that dominated Early Cenozoic deformation to the modern structural regime is related to eastward migration of the eastern plateau margin into an area of weak lower crust beneath eastern Tibet. This resulted in merging of two regions of weak crust and in rapid eastward flow within the deep crust.

Epilogue

On 12 May 2008, a magnitude 7.9 earthquake occurred near the town of Wenchuan, China (*46*) (Fig. 6). Rupture propagated for ~270 km along north-northeast striking, west-dipping fault(s) with up to ~10 m of thrust- and right-slip displacement. The hypocenter of the main event is estimated at ~10- to 20-km depth, but details of the surface rupture and slip distribution remain under investigation.

The main event and aftershocks occurred beneath the steep margin of the Tibetan plateau, adjacent to the mechanically strong Sichuan Basin and near profile 3a (Fig. 5), where GPS data reveal up to several millimeters per year convergence and right-slip. A geological section through the epicenter shows an imbricate thrust sequence, emplaced above the Pengguan massif in Jurassic time. These units were refolded and thrust eastward in Late Cenozoic time. The basal thrust fault roots westward into the basement beneath the Pengguan massif. Folded strata can be matched across the Cenozoic faults, which do not appear to have large displacement, perhaps several tens of kilometers in total. Initial rupture during the Wenchuan earthquake probably occurred along a ramp in the basal thrust or related faults (*46*) (Fig. 6).

From information currently available and from the arguments presented here, we propose that along the steep Longmen Shan margin (i) active thrust faulting serves mainly to accommodate vertical uplift of the plateau margin, with crustal thickening occurring by lateral injection of weak crust (Fig. 5), and (ii) the right-slip component of displacement serves to flux upper-crustal material northeastward around the strong lithosphere of the Sichuan Basin. Ongoing study of postseismic displacements related to the Wenchuan earthquake of 12 May 2008 should provide much data to test hypotheses of flow and deformation in the deep crust beneath eastern Tibet.

References and Notes

1. E. Argand, *Cong. Geol. Int.* **1922**, 171 (1922).
2. P. Tapponnier, G. Peltzer, R. Armijo, *Geol. Soc. London Spec. Publ.* **19**, 115 (1986).
3. P. Tapponnier *et al*., *Science* **294**, 1671 (2001).
4. G. A. Houseman, P. C. England, *J. Geophys. Res.* **91**, 3651 (1986).
5. P. Kapp, P. G. DeCelles, G. E. Gehrels, M. Heizler, L. King, *Geol. Soc. Am. Bull.* **119**, 917 (2007).
6. P. Molnar, P. C. England, J. Martinod, *Rev. Geophys.* **31**, 357 (1993).
7. D. B. Rowley, *J. Geol.* **106**, 229 (1998).
8. P. G. DeCelles, D. M. Robinson, G. Zandt, *Tectonics* **21**, 1062, 10.1029/2001TC001322 (2002).
9. L. Shu, X. Zhou, P. Deng, W. Zhu, *Acta Geol. Sin.* **81**, 573 (2007).
10. Z. Liu, C. Wang, H. Yi, *J. Sed. Res.* **71**, 971 (2001).
11. E. Cowgill, A. Yin, M. Harrison, *J. Geophys. Res.* **108**, 2346, 10.1029/2002JB002080 (2003).
12. B. Meyer *et al*., *Geophys. J. Int.* **135**, 1 (1998).
13. D. S. Rowley, B. S. Currie, *Nature* **439**, 677 (2006).
14. S. Akciz, B. C. Burchfiel, J. L. Crowley, J. Yin, L. Chen, *Geosphere* **4**, 292 (2008).
15. E. S. Holbig, T. L. Grove, *J. Geophys. Res.* **113**, B04210, 10.1029/2007JB005149 (2008).
16. R. van der Hilst, T. Seno, *Earth Planet. Sci. Lett.* **120**, 395 (1993).
17. R. Hall, C. K. Morley, in *Continental-Ocean Interactions Within East Asian Marginal Seas*, P. Clift, W. Kuhnt, P. Wang, D. Hayes, Eds., *AGU Geophys. Monogr.* **149**, pp. 55–85 (2004).
18. J.-C. Sibuet, S. K. Hsu, E. Debayle, in *Continental-Ocean Interactions Within East Asian Marginal Seas*, P. Clift, W. Kuhnt, P. Wang, D. Hayes, Eds., *AGU Geophys. Monogr.* **149**, pp. 127–158 (2004).
19. E. Honza, H. Tokuyama, S. Wonn, in *Continental-Ocean Interactions Within East Asian Marginal Seas*, P. Clift, W. Kuhnt, P. Wang, D. Hayes, Eds., *AGU Geophys. Monogr.* **149**, pp. 87–108 (2004).
20. C. Li, R. D. van der Hilst, A. S. Meltzer, E. R. Engdahl, *Earth Planet. Sci. Lett.*, 10.1016/j.epsl.2008.07.016 (2008).
21. C. Li, R. D. van der Hilst, E. R. Engdahl, S. Burdick, *Geochem. Geophys. Geosyst.*, 10.1029/2007GC001806 (2008).
22. P.-Z. Zhang *et al*., *Geology* **32**, 809 (2004).
23. E. Wang *et al*., *Geol. Soc. Am. Spec. Publ.* **327**, 108 (1998).
24. B. J. Meade, *Geology* **35**, 81 (2007).
25. R. Zhou *et al*., *Acta Geol. Sin.* **81**, 593 (2007).
26. B. C. Burchfiel, *GSA Today* **14**, 4 (2004).
27. B. C. Burchfiel *et al*., *Geology* **17**, 748 (1989).
28. B. C. Burchfiel, Z. Chen, Y. Liu, L. H. Royden, *Int. Geol. Rev.* **37**, 661 (1995).
29. H. Williams, S. Turner, S. Kelley, N. Harris, *Geology* **29**, 339 (2001).
30. P. M. Blisniuk *et al*., *Nature* **412**, 628 (2001).
31. P. C. England, G. A. Houseman, *J. Geophys. Res.* **94**, 17561 (1989).
32. K. L. Cook, L. H. Royden, *J. Geophys. Res.*, 10.1029/2007JB005457 (2008).
33. M. K. Clark *et al*., *J. Geophys. Res.* **111**, 10.1029/2005JF000294 (2006).
34. M. K. Clark *et al*., *Geology* **33**, 525 (2005).
35. W. Ouimet, thesis, Massachusetts Institute of Technology (2007).
36. E. Kirby *et al*., *Tectonics* **21**, 1001, 10.1029/2000TC001246 (2002).
37. L. M. Flesch, A. J. Haines, W. E. Holt, *J. Geophys. Res.* **106**, 16435 (2001).
38. M. K. Clark, L. H. Royden, *Geology* **28**, 703 (2000).
39. K. D. Nelson *et al*., *Science* **274**, 1684 (1996).
40. H. Yao, R. D. van der Hilst, M. V. de Hoop, *Geophys. J. Int.* **166**, 732 (2006).
41. H. Yao, C. Beghein, R. D. van der Hilst, *Geophys. J. Int.* **173**, 205 (2008).
42. L. Xu, S. Rondenay, R. D. van der Hilst, *Phys. Earth Planet. Inter.* **165**, 176 (2007).
43. L. H. Royden, *J. Geophys. Res.* **101**, 17679 (1996).
44. F. Shen, L. H. Royden, B. B. C. Burchfiel, *J. Geophys. Res.* **106**, 6793 (2001).
45. Profile A: Crust added east of the profile (after 15 Ma) is ~2.4×10^7 km^3. Profile B: Crust added south of the profile (after 15 Ma) is ~1.5×10^7 km^3. Upper-crustal viscosity (and whole-crust viscosity under steep plateau margins) is 10^{20} to 10^{21} Pa s; deep crustal channel thickness is assumed to be 20 km and its viscosity is 10^{16} to 10^{17} Pa s beneath the high plateau and 10^{18} Pa s beneath the southeastern and northeastern plateau margins.
46. B. C. Burchfiel *et al*., *GSA Today* **18**, 4 (2008).
47. The tomographic cross sections depict wave speed perturbations relative to a laterally homogeneous reference Earth model and show slow seismic-wave propagation in parts of the crust and mantle lithosphere. The *P*-wave speed model is obtained from travel-time tomography (*20*, *21*); the *S*-wave speed model is obtained from surface-wave array tomography (*40*, *41*).
48. U.S. Geological Survey Earthquake Center, http://earthquake.usgs.gov/eqcenter/eqinthenews/2008/us2008ryan.
49. E. R. Engdahl, R. D. van der Hilst, R. P. Buland, *Bull. Seismol. Soc. Am.* **88**, 722 (1998).

50. This project has been supported by NSF Earth Science, Continental Dynamics Program since 1986, most recently by grant EAR-0003571. This work would not have been possible without the collaboration and support of our colleagues at the Chendu Institute of Geology and Mineral Resources over many years, especially Chen Zhiliang, and at the Geological Institute of Yunnan, in Kunming.

10.1126/science.1155371